Thin Solid Films 593 (2015) 110–115

Contents lists available at ScienceDirect

Thin Solid Films

journal homepage: www.elsevier.com/locate/tsf

Study of the structure of titanium thin films deposited with a vacuum arc as a function of the thickness

M. Fazio [a], D. Vega [b], A. Kleiman [a], D. Colombo [c], L.M. Franco Arias [a], A. Márquez [a,*]

[a] Instituto de Física del Plasma, CONICET and Departamento de Física, Facultad de Ciencias Exactas y Naturales, Universidad de Buenos Aires, Cdad. Universitaria Pab. 1, 1428 Buenos Aires, Argentina
[b] Departamento Física de la Materia Condensada, Gerencia de Investigación y Aplicaciones, Comisión Nacional de Energía Atómica, Av. Gral Paz, 1499 San Martín, Buenos Aires, Argentina
[c] División Metalurgia INTEMA, CONICET/UNMdP, Av. J. B. Justo 4302, B7608FDQ Mar del Plata, Argentina

ARTICLE INFO

Article history:
Received 12 December 2014
Received in revised form 22 July 2015
Accepted 9 September 2015
Available online 11 September 2015

Keywords:
Titanium
Thin films
Films
Face centered cubic titanium phase
Vacuum arc discharge

ABSTRACT

Polycrystalline titanium thin films have been widely employed as interlayer between the substrate and different coatings in order to improve adhesion strength, corrosion resistance and wear performance, as well as to promote the growth of crystalline phases of the coating. The thickness of the Ti layer can be relevant on the behavior of the coatings, however very few studies have been carried out. In this work, the crystal structure of polycrystalline titanium films deposited with a vacuum arc discharge on monocrystalline silicon wafers (100) was studied and a dependence on the film thickness was found. The presence of the fcc phase of titanium was observed for the thinnest films with a critical thickness estimated in 300 nm, a much larger value than those reported for other deposition processes. For larger thicknesses, the films grew as α-titanium with a preferred orientation in the [100] direction. The obtained results agreed with a growth model based on the matching between the film and the substrate lattice. The characteristics of the films deposited in two steps, which had not been previously investigated, reinforced the suggested model.

1. Introduction

Polycrystalline titanium thin films have been widely employed as interlayer between the substrate and different coatings, on metallic, semiconductor or ceramic substrates and for metallic, metallic compounds or carbon coatings. The Ti interlayer has been included in order to improve adhesion strength, corrosion resistance and wear performance, as well as to promote the growth of crystalline phases of the coating [1–3]. In some works the influence of the Ti interlayer thickness on the properties of multilayer systems has been analyzed, the thickness of the Ti layer being relevant on the behavior of the coatings. However, very few studies about the dependence of the characteristics of Ti films on the thickness have been carried out.

At ambient condition, Ti is in the hexagonal-close-packed (hcp) crystal structure, which is referred to as α phase. This structure transforms to a body-centered-cubic (bcc) structure, called β phase, when the temperature is higher than 1155 K. At room temperature, the α phase transforms to the hexagonal ω phase (three atoms per unit cell) when the pressure is increased between 2 and 9 GPa. Other two high pressure phases, γ-Ti (distorted hcp) and δ-Ti (distorted bcc), have been found. At room temperature, the phase transition from ω-Ti to γ-Ti occurs at 116 GPa, and into δ phase at 140 GPa [4].

The face centered cubic (fcc) Ti phase has been only found in thin films and in high energy milled powder. Wawner Jr. and Lawless were the first to report the fcc Ti phase in Ti films epitaxially grown on NaCl single crystals [5]. Afterwards, some investigations about epitaxial growth of Ti thin films on metallic substrates and on semiconductors have been published (e.g. Al [6,7] and SiC [8]). In all cases, at the onset of the growth the Ti atomic structure presented the fcc phase, which seemed to perfectly match the substrate lattice in the directions parallel to the surface plane. At a critical thickness the hcp phase appeared, this being the predominant phase for thicker films. The reported critical thickness values varied from 1 to 20 nm for epitaxial growth. Beyond this thickness, axial alignment with the substrate was only partially preserved, and off-normal alignment was lost. The disorder in the film at coverage larger than the critical thickness was associated with the formation of misfit dislocations or the relaxation to the hcp phase of Ti [6]. More recently, a study of the dependence of the crystalline structure on the thickness in polycrystalline Ti films deposited on Si substrates by DC magnetron sputtering has been presented [9]. The authors analyzed the structure, textures and stresses of Ti films with thickness in the range of 140–720 nm. In that work, from the deconvolution of Ti X ray diffraction peaks the fcc and hcp phases were detected in the thinnest films, while for films with a thickness larger than 500 nm only the hcp phase was identified. They suggested that fcc Ti is locally stable in highly stressed hcp Ti matrix at relatively low thin film thicknesses.

In view of the lack of information about the crystal structure of polycrystalline Ti films deposited with vacuum arcs on monocrystalline

* Corresponding author.
E-mail address: amarquez@df.uba.ar (A. Márquez).

http://dx.doi.org/10.1016/j.tsf.2015.09.015
0040-6090/

silicon wafers (100) as a function of the film thickness, a systematic study on this subject was carried out. The structure, the morphology and the residual stresses of the films were studied. Characteristics of films deposited in one and two steps were compared.

2. Experimental details

The system employed to produce the cathodic arc discharge had a high power DC source (model ARCC 18KW 150 A, ALTATEC) connected to a titanium cathode and to a grounded annular copper anode. In Fig. 1 a schematic view of the complete device is shown. The cathode was a cylinder of 55 mm in diameter and 40 mm thick, the anode had an internal diameter of 80 mm and was electrically insulated from the cathode and the vacuum chamber. The vacuum chamber consisted of a stainless steel cylinder (50 cm long, 10 cm internal diameter). The vacuum system was made up of a diffusion pump assisted by a rotary vane pump that reached a base pressure lower than 10^{-6} Pa. The anode and the cathode had water cooling. In order to initiate the discharge, an auxiliary electrode (trigger) in contact with the cathode was used. The discharges were run at a current of 110 A and discharge voltage was 25 V. The pressure during the discharges remained lower than 10^{-6} Pa.

The employed substrates were monocrystalline silicon wafers (100) doped with boron with a surface area of 20×20 mm^2 and 375 μm thick. Samples were located facing the cathode on a grounded holder at a distance of 300 mm. The samples were exposed to the discharge for times ranging from 30 to 180 s, in one or two steps. For samples grown on two steps, there was an average waiting time of 15 min between steps while maintaining the chamber pressure below 10^{-6} Pa.

The thickness of the films was determined by cleaving the samples and studying the profile by scanning electron microscopy (SEM), using a microscope Philips 515 with an Oxford Instruments INCA Energy 250 with a Si(Li) detector (10 mm^2 in area) for electron dispersive spectroscopy (EDS).

The films were characterized by X-ray reflectivity (XRR) in order to estimate their density. The measurements were performed in the D10A-XRD2 beamline of the National Synchrotron Light Source (LNLS), Campinas, Brazil, using an X-ray energy of 8 keV (λ = 0.1549 nm). The opening of the slit that defined the vertical size of the incident X-ray beam was 100 μm, located at 40 cm from the sample. A Mythen linear detector was placed at 100 cm from the sample with a 100 μm width slit. For films with thicknesses lower than 200 nm, a θ–2θ scan was performed varying the angle of incidence with respect to the surface from 0.1° to 2°. For films with thicknesses above 200 nm no oscillations were noticeable in the XRR pattern, so a diffuse scattering measurement (rocking scan) was employed.

The crystalline structure was analyzed by X ray diffraction (XRD) in Bragg–Brentano geometry. The diffractograms were measured using a Panalytical diffractometer Empyrean model with a CuKα source with a PixCel 3D detector. For this source the X ray intensity is 90% attenuated in a length of 1.1 μm of titanium. The angle 2θ was varied between 30° and 135°, avoiding the peak corresponding to silicon in $2\theta = 60°$ so as not to saturate the detector. The presence of macrostrains in the films was studied by the $\sin^2\psi$ method using a Panalytical X'Pert PRO diffractometer with a CuKα source.

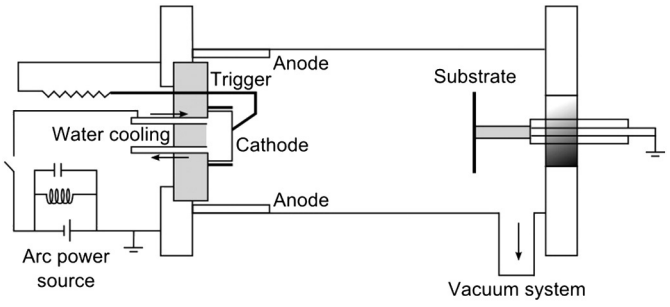

Fig. 1. Schematic view of the cathodic arc discharge system employed to grow the films.

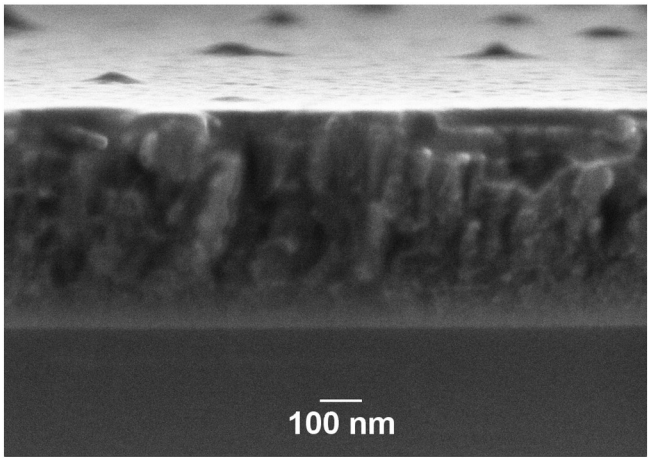

Fig. 2. Typical SEM image of a film depth profile.

3. Results

Fig. 2 corresponds to a typical image of the depth profile obtained by SEM for a film grown in a single discharge. The films displayed a compact columnar structure, with a column width of ~100 nm. The thickness of all the films was measured from images similar to that of Fig. 2, the growth rate resulting in (3.8 ± 0.3) nm/s. EDS compositional analysis indicated a minimum contamination of oxygen and carbon, and a titanium content higher than 80%.

The mass density of the films was estimated from the critical angle observed in XRR measurements. The critical angle was determined by fitting the interference maxima and minima by the modified Bragg equation when the θ–2θ scan was employed [10]; and from the position of the Yoneda peaks when the rocking scan was used [11]. In all cases the critical angle was estimated with an uncertainty of ~5%, the mass density of all the films was found to be in the range (4.3 ± 0.2) 10^3 kg/m^3.

The crystalline structure of the films was studied by XRD, the deposition time and the thickness for the presented samples are shown in Table 1. Fig. 3a shows the diffractograms of films with different thicknesses grown in a single discharge, and Fig. 3b presents a detail of the main peaks for 2θ between 33° and 45°. The diffractogram registered for the silicon substrate and the tabulated peak positions corresponding to α-titanium are also included in Fig. 3.

For films (i) and (ii), no peaks corresponding to α-titanium were noted. Only one peak was observed at $2\theta = (37.05 \pm 0.03)°$ which cannot be attributed to the substrate or any other titanium compound (such as oxides or nitrates). The interplanar spacing associated with this peak was (2.424 ± 0.007) Å. Film (ii) also exhibited one additional peak at $2\theta = (78.75 \pm 0.03)°$. The corresponding interplanar spacing was (1.214 ± 0.007) Å, half the spacing associated with the previously mentioned peak. This indicated that both peaks correspond to the same crystallographic direction. This diffractogram was consistent with the reported fcc-titanium structure [9], therefore the peak

Table 1
Features of the films studied by SEM and XRD.

Sample label	Number of discharges	Total deposition time [s]	Thickness [nm]
(i)	1	30	115
(ii)	1	60	220
(iii)	1	120	430
(iv)	1	150	515
(v)	2	60 (2 × 30)	240
(vi)	2	180 (2 × 90)	750

observed at $2\theta = (37.05 \pm 0.03)°$ could be indexed as (111) while the peak at $2\theta = (78.75 \pm 0.03)°$ corresponded to (222). The lattice parameter of the fcc-titanium calculated from the diffraction peaks was (4.200 ± 0.006) Å, which was in good agreement with the parameters reported and calculated for this phase [12]. For a polycrystalline fcc structure, reflections from other crystallographic planes should have been observed. The fact that no other peaks from fcc-titanium have been noticed indicated that this phase grew only in the [111] direction. The (111) texture of the films was also corroborated by X ray diffraction pole figure analysis. The lattice parameter obtained for fcc-titanium films permitted calculation of the film density for this phase resulting in $(4.29 \pm 0.02)\ 10^3$ kg/m^3. This value lay within the density interval

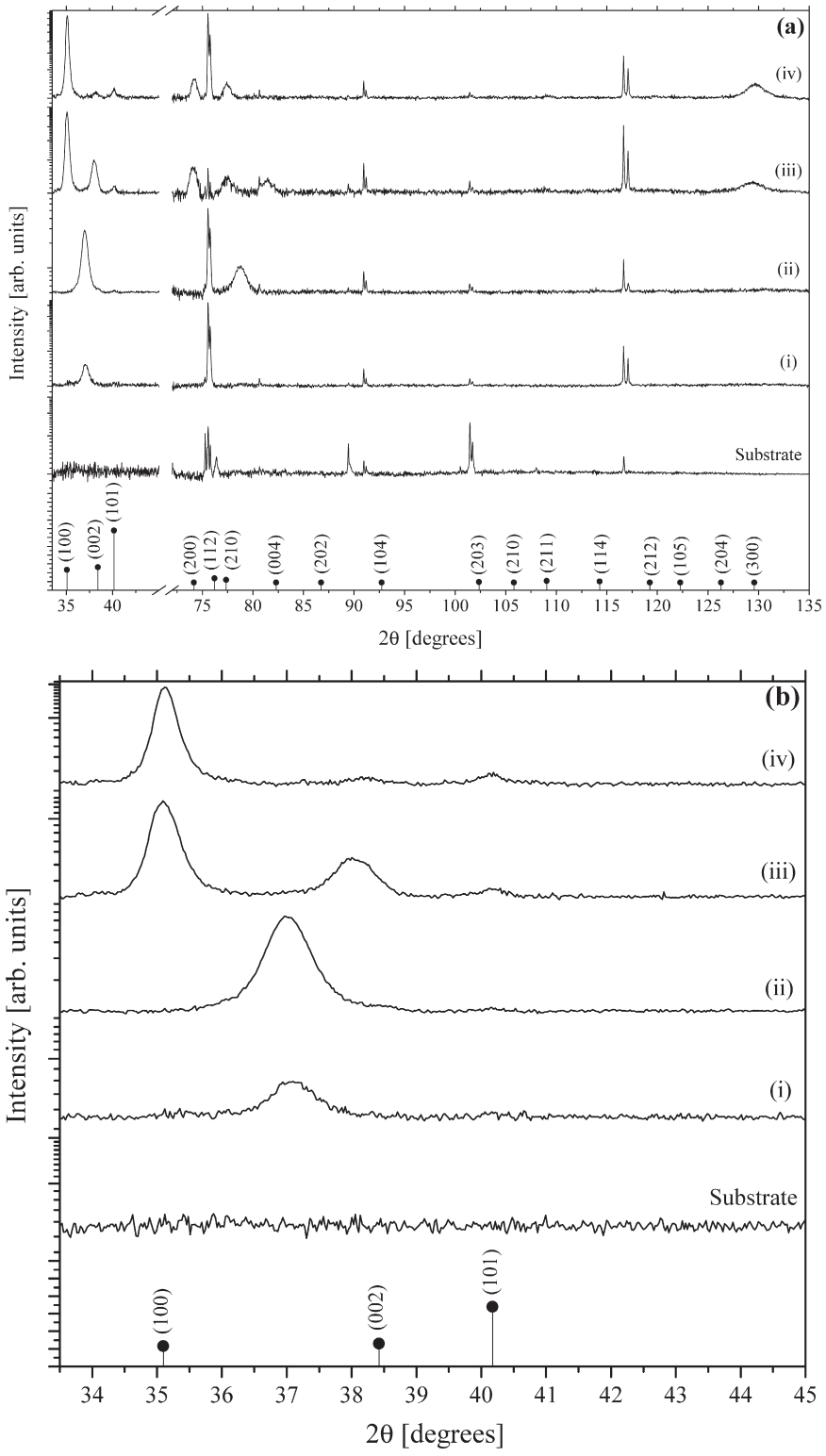

Fig. 3. XRD diffractograms of films grown in a single discharge with different duration. (a) Total 2θ measured range and (b) detail for 2θ between 33° and 45°. The tabulated peak positions corresponding to α-titanium are indicated.

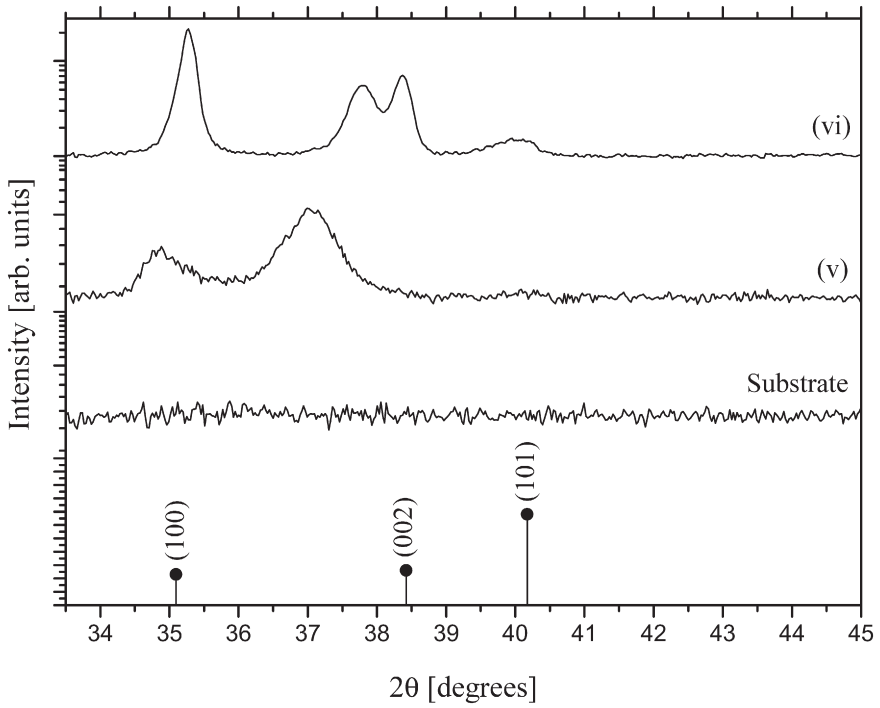

Fig. 4. XRD diffractograms of films grown in two discharges with different duration for 2θ between 33° and 45°. The tabulated peak positions corresponding to α-titanium are indicated.

determined from XRR measurements; the experimental uncertainty not making possible to distinguish the difference in the density between the fcc and the hcp phases.

On the other hand, for samples (iii) and (iv) no peaks corresponding to fcc-titanium were observed, the α-titanium being the only phase present in the films. Therefore, the critical thickness for obtaining fcc-titanium in this process was above 220 nm and below 430 nm (~300 nm). In sample (iii) all the main peaks from the α-titanium phase can be noticed. When the thickness increased (sample (iv)), peaks with contributions in the [100] direction did not change significantly while peaks (002) and (004) decreased their intensity. In films (iii) and (iv), the (100) and (300) peaks had a relative intensity higher than the tabulated values. These features were consistent with a preferred orientation in the [100] direction. It is worth noting that the peaks (002) and (004) showed a shift from their tabulated position of ~0.26° and ~0.49°, respectively.

Films were also grown with two discharges of equal duration each. Fig. 4 shows the diffractograms in Bragg–Brentano geometry of two such films for 2θ between 33° and 45°. Both films exhibited the peak associated with the fcc-titanium phase and the α-titanium peaks with a preferred orientation in the [100] direction. The peak associated with fcc-titanium for film (vi) showed a shift of ~0.75° in its position, which indicated a variation of around 2% in the lattice parameter in comparison to the parameter estimated above.

The crystallite size and the presence of microstrain in the samples were analyzed from the diffractograms by the Scherrer equation [13]. All detected peaks in the diffractograms were fitted by a Lorentzian function. Fig. 5 presents a typical fit for (111) fcc peak and (100) α-titanium peak from films grown in one discharge.

According to the Scherrer equation, the integral breadth (w) relates to the crystallite size (L) and the root mean square value of the microstrain ($<\varepsilon^2>^{1/2}$) as:

$$w\cos\theta = K\lambda/L + 2<\varepsilon^2>^{1/2}\sin\theta$$

with $K = 0.94$ as a dimensionless number known as the Scherrer constant and λ as the x-ray wavelength. The instrumental integral

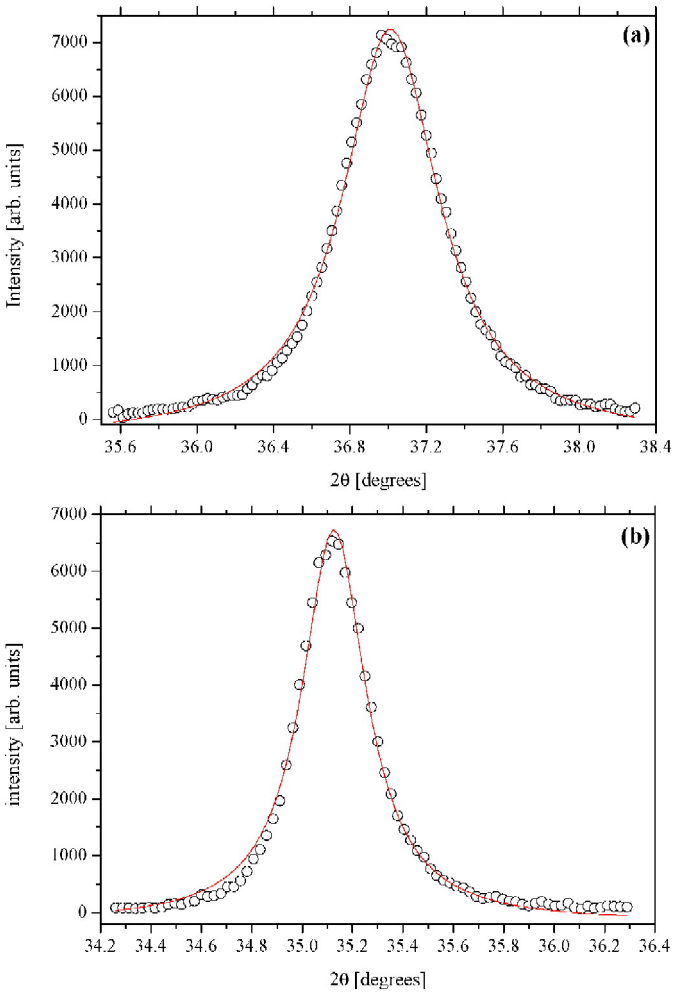

Fig. 5. Typical fits for (a) fcc and (b) α-titanium peaks by a Lorentzian function.

breadth (w_{inst}) was estimated from a silicon sample peak as (0.077 ± 0.005)°. So the peak integral breadth was calculated as $w = \omega - w_{inst}$, with ω as the integral breadth obtained from the Lorentzian fit. The presence of microstrain was not appreciable for fcc or α-titanium due to the fact that wcosθ did not show any significant dependence with sinθ. Therefore the only contribution to the peak broadening was due to crystallite size. The crystallite size corresponding to all the peaks observed for fcc-titanium resulted in ~10 nm, while for α-titanium the crystallite size was ~20 nm.

The presence of macrostrain in the films was studied for the α-titanium phase by analyzing the (300) peak in films (iii), (iv) and (vi). Fcc-titanium films could not be studied by this method because of the lack of peaks at high angles. In all cases, the stresses in the α-titanium phase were found to be tensile and were estimated in 0.3 GPa. The tensile stress is generally associated to a film density lower than the tabulated value for the bulk [14]. The expected decrease in the film density according to the observed stress lay within the experimental uncertainty associated to the measured density.

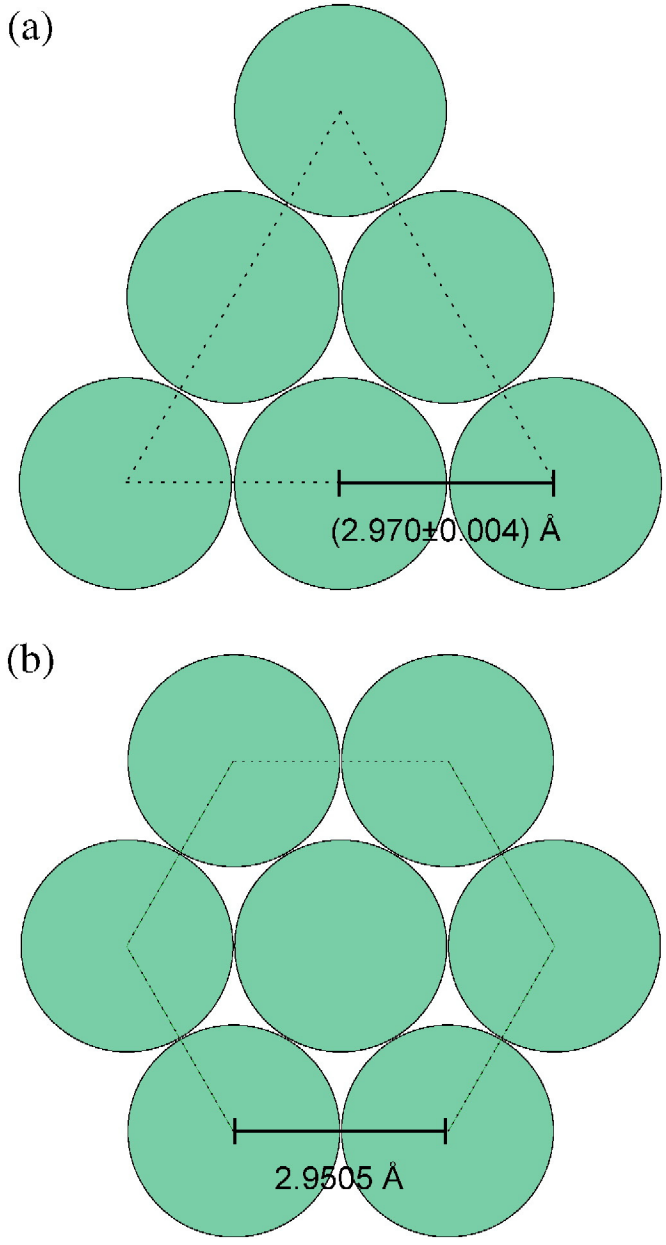

Fig. 6. Schematic representation of (a) the (111) surface of fcc-titanium and (b) the (002) surface of α-titanium. The corresponding interatomic distances are indicated.

4. Discussion

Based on XRD results and regarding the structure of the fcc and hcp lattices, the phase transformation could be analyzed. Fig. 6a shows the (111) surface of fcc-titanium with the corresponding interatomic distance obtained from the experimental interplanar spacing. The titanium atoms are represented with their corresponding metallic radius. The (111) fcc surface is equivalent to the (002) surface of α-titanium, depicted in Fig. 6b, except for the difference in stacking associated to the fcc and hcp lattices. The interatomic distances of the surfaces differ in less than 1% between them and both structures are closed-packed. It is important to remark that the initial stage of the growth is regarded as a different phase of titanium, and cannot be attributed to an hcp lattice under strain. If the observed peaks were identified as reflections from a stressed hcp lattice, the resulting lattice parameters would show a variation of around 4% from the tabulated values for α-titanium, and the necessary strain to produce such a significant stress would be much higher than the reported yield strains for thin films [15].

Taking into account that the crystalline phase of the films was found to be dependent upon its thickness, the phase formation during film growth can be explained based on the matching between the film and the substrate lattice. The films initially grow in the fcc-titanium phase which is the most compact orientation and stacking, possibly as a way to reduce the interfacial energy with the substrate. In a later stage of the film growth, faults that allow for a phase transition to the hcp lattice are introduced. This was evidenced in sample (iii) which displayed a large shift in the position of the (002) peak. Finally, beyond the critical thickness, the film continued to grow as α-titanium with a preferred orientation in the [100] direction. The results obtained in the present work for films deposited with two discharges supported the proposed growth process. Although the total thickness of film (v) was lower than the critical value and each layer was similar in thickness to film (i), which presented only fcc-titanium, the α-titanium phase was also present. In the case of film (vi), although the total thickness was larger than that of film (iv) where only α-titanium was detected, the fcc phase was also present. The structure of these films can be explained by the fact that only the growth of the first layer would have been influenced by the substrate favoring the fcc phase while the usual α-titanium structure could be associated to the subsequent layer. The fcc-titanium structure was present for films grown in two steps because the thickness of the first layer was lower than the critical value. The observed change in the fcc-titanium lattice parameter for film (vi) could be due to the stresses introduced in the structure by faults, as the layer thickness was close to the critical value where the transition to α-titanium is expected.

It is worth noting that the critical thickness for fcc-titanium growth found in this work (~300 nm) was significantly larger than the values obtained for other deposition processes. Critical thicknesses from a few monolayers up to 20 nm were reported for films epitaxially grown [5,6]. For polycrystalline Ti films deposited on Si (100) by sputtering, Chakraborty et al. [9] determined that the critical thickness was lower than 140 nm. In addition, these films grown by sputtering showed a preferred orientation in the [002] direction for α-titanium. For the films studied in the present work the preferred orientation was found to be in the [100] direction despite employing the same substrate. Thus, the critical thickness associated to the fcc phase and the preferred orientation for α-titanium seemed to depend on the deposition process.

The presence of the fcc phase has been previously analyzed using a thermodynamical approach based on the estimation of the change in free energy of Ti (ΔG) when it transforms from fcc to α-titanium, as proposed in [9,16]. The total free energy change has three main contributions: the change in bulk free energy, the change in elastic strain energy, and the change in surface free energy. Only the first one contributes significantly to ΔG as it is an order of magnitude higher than the other two, taking into account the measured strain and the

corresponding surface energies. The change in bulk free energy is positive, implying that the transformation could not be possible. Van Heerden et al. [17] also used a similar calculation for ΔG in multilayer Al-Ti films, and concluded that the transformation seems not to be energetically possible. Nevertheless, the fcc phase has been observed for a variety of films and different critical thicknesses have been measured for different growth processes. The thermodynamical approach used so far is not appropriate given the fact that the growth of a film is a dynamic process and this calculation of ΔG does not take into account in any way the growth process.

5. Conclusions

The crystal structure of polycrystalline titanium films deposited with a vacuum arc discharge on monocrystalline silicon wafers (100) was found to depend on the film thickness. The presence of the fcc phase of titanium was observed for the thinnest films. The critical thickness was estimated in 300 nm, a much larger value than those reported for other deposition processes. For larger thicknesses, the films grew as α-titanium with a preferred orientation in the [100] direction. The obtained results agreed with the proposed growth model: the fcc-titanium formation is influenced by the substrate structure, and the transformation fcc–hcp is induced by the development of faults as the thickness increases. The characteristics of the films deposited in two steps, which had not been previously investigated, reinforced the suggested model.

Acknowledgments

This work was supported by grants from Universidad de Buenos Aires (PID 20020110100161) and CONICET (PIP 11220120100468CO). XRR measurements were performed at LNLS (under proposal XRD1-13700 - (XRD2)).

References

[1] E. Vassallo, R. Caniello, A. Cremona, D. Dellasega, E. Miorin, Titanium interlayer to improve the adhesion of multilayer amorphous boron carbide coating on silicon substrate, Appl. Surf. Sci. 266 (2013) 170–175.
[2] B. Zhou, X. Jiang, A.V. Rogachev, D. Sun, X. Zang, Growth and characteristics of diamond-like carbon films with titanium and titanium nitride functional layers by cathode arc plasma, Surf. Coat. Technol. 223 (2013) 17–23.
[3] D.S. Rama Krishna, Y. Sun, Z. Chen, Magnetron sputtered TiO_2 films on a stainless steel substrate: selective rutile phase formation and its tribological and anti-corrosion performance, Thin Solid Films 519 (2011) 4860–4864.
[4] D. Errandonea, Y. Meng, M. Somayazulu, D. Häusermann, Pressure-induced $\alpha \rightarrow \omega\alpha \rightarrow \omega$ transition in titanium metal: a systematic study of the effects of uniaxial stress, Phys. B Condens. Matter 355 (2005) 116–125.
[5] F.E. Wawner Jr., K. Lawless, Epitaxial growth of titanium thin films, J. Vac. Sci. Technol. 6 (1969) 588–590.
[6] A.A. Saleh, V. Shutthanandan, N.R. Shivaparan, R.J. Smith, T.T. Tran, S.A. Chambers, Epitaxial growth of fcc Ti films on Al(001) surfaces, Phys. Rev. B 56 (1997) 9841–9847.
[7] S.K. Kim, F. Jona, P.M. Marcus, Growth of face-centred-cubic titanium on aluminium, J. Phys.: Condens. Matter 8 (1996) 25–36.
[8] Y. Sugawara, N. Shibata, S. Hara, Y. Ikuhara, Interface structure of face-centered-cubic-Ti thin film grown on 6H–SiC substrate, J. Mater. Res. 15 (2000) 2121–2124.
[9] J. Chakraborty, K. Kumar, R. Ranjan, S. GhoshChowdhury, S.R. Singh, Thickness-dependence fcc–hcp phase transformation in polycrystalline titanium thin films, Acta Mater. 59 (2011) 2615–2623.
[10] A. Kleiman, D.G. Lamas, A.F. Craievich, A. Márquez, X-Ray reflectivity analysis of titanium dioxide thin films grown by cathodic arc deposition, J. Nanosci. Nanotechnol. 14 (2014) 3902–3909.
[11] S.K. Sinha, E.B. Sirota, S. Garoff, H.B. Stanley, X-ray and neutron scattering from rough surfaces, Phys. Rev. B 38 (1988) 2297–2311.
[12] A. Aguayo, G. Murrieta, R. de Coss, Elastic stability and electronic structure of fcc Ti, Zr, and Hf: a first-principles study, Phys. Rev. B 65 (2002) 092,106.
[13] J.I. Langford, A.J.C. Wilson, Scherrer after sixty years: a survey and some new results in the determination of crystallite size, J. Appl. Crystallogr. 11 (1978) 102–113.
[14] K.H. Müller, Stress and microstructure of sputter-deposited thin films: molecular dynamics investigations, J. Appl. Phys. 62 (1987) 1796–1799.
[15] W.D. Nix, Mechanical properties of thin films, Metall. Mater. Trans. A 20 (1989) 2217–2245.
[16] P.M. Marcus, F. Jona, Identification of metastable phases: face-centred cubic Ti, J. Phys. Condens. Matter 9 (1997) 6241–6246.
[17] D. Van Heerden, D. Josell, D. Shechtman, The formation of f.c.c. titanium in titanium-aluminium multilayers, Acta Mater. 44 (1996) 297–306.